

1 Article

2 **Investigation of trace and critical elements (including**  
3 **actinides) in flotation sulphide concentrates of**  
4 **Kassandra mines (Chalkidiki, Greece)**

5 **Evangelos Tzamos<sup>1,\*</sup>, Argyrios Papadopoulos<sup>2</sup>, Giovanni Grieco<sup>3</sup>, Stylianos Stoulos<sup>4</sup>, Micol**  
6 **Bussolesi<sup>3</sup>, Emmanouil Daftsis<sup>2</sup>, Eleftheria Vagli<sup>2</sup>, Dimitrios Dimitriadis<sup>2</sup> and Athanasios**  
7 **Godelitsas<sup>1</sup>**

8 <sup>1</sup> Department of Geology and Geoenvironment, National and Kapodistrian University of Athens, Zografou  
9 Campus, 15784, Athens (Greece); etzamos@geol.uoa.gr; agodel@geol.uoa.gr

10 <sup>2</sup> Hellas GOLD S.A., V. Sofias 23A Av., 10674 Athens & 63082Stratoni, Chalkidiki(Greece);  
11 Argyris.Papadopoulos@gr.eldoradogold.com; Emmanouil.Daftsis@gr.eldoradogold.com;  
12 Eleftheria.Vagli@gr.eldoradogold.com; Dimitris.Dimitriadis@gr.eldoradogold.com

13 <sup>3</sup> Department of Earth Sciences, UniversitàdegliStudi di Milano, via Botticelli n.23, 20133, Milano (Italy);  
14 giovanni.grieco@unimi.it; micol.bussolesi@unimi.it

15 <sup>4</sup> Department of Physics, AristotleUniversity of Thessaloniki, University Campus, 54124, Thessaloniki  
16 (Greece); stoulos@auth.gr

17 \* Correspondence: etzamos@geol.uoa.gr

18 Received: date; Accepted: date; Published: date

19 **Abstract:** Pyrite/As-pyrite/arsenopyrite (Py-(As)Py-AsPy), galena (PbS) and sphalerite (ZnS)  
20 concentrates from the flotation plants of Olympiada and Stratoni (Kassandra mines, Chalkidiki, N.  
21 Greece) have been investigated for their trace and critical element content, including actinides  
22 associated to natural radioactivity. It has been revealed that except Pb, Zn, Ag, and Au, being  
23 exploited by Hellas Gold S.A., there are also significant concentrations of Sb and Ga (Sb: >0.2 wt.%  
24 in PbS concentrate; Ga: 25 ppm in ZnS concentrate), but no considerable contents of Bi, Co, V, and  
25 REE. Concerning other elements, As is found in elevated concentrations (> 1 wt.% in  
26 Py-(As)Py-AsPy Olympiada concentrate and almost 1 wt.% in Stratoni PbS and ZnS concentrates)  
27 together with Cd (specifically in ZnS concentrate). However, it has been postulated, for first time in  
28 the literature, that actinides occur in very low concentrations (U<2 ppm and Th<0.5 ppm in all  
29 examined concentrates), eliminating the possibility of natural radioactivity in the Hellas Gold S.A.  
30 products. The concentrations of the natural radionuclides (<sup>238</sup>U, <sup>232</sup>Th and <sup>40</sup>K) are much lower  
31 compared to commercial granitic rocks. Thus, the associated radioactive dose is insignificant and it  
32 can be assumed that no risk concerning natural radionuclides contamination of surface and  
33 underground waters is present.

34 **Keywords:** Kassandra mines; Chalkidiki; sulphide ores; flotation concentrates; critical elements;  
35 actinides  
36

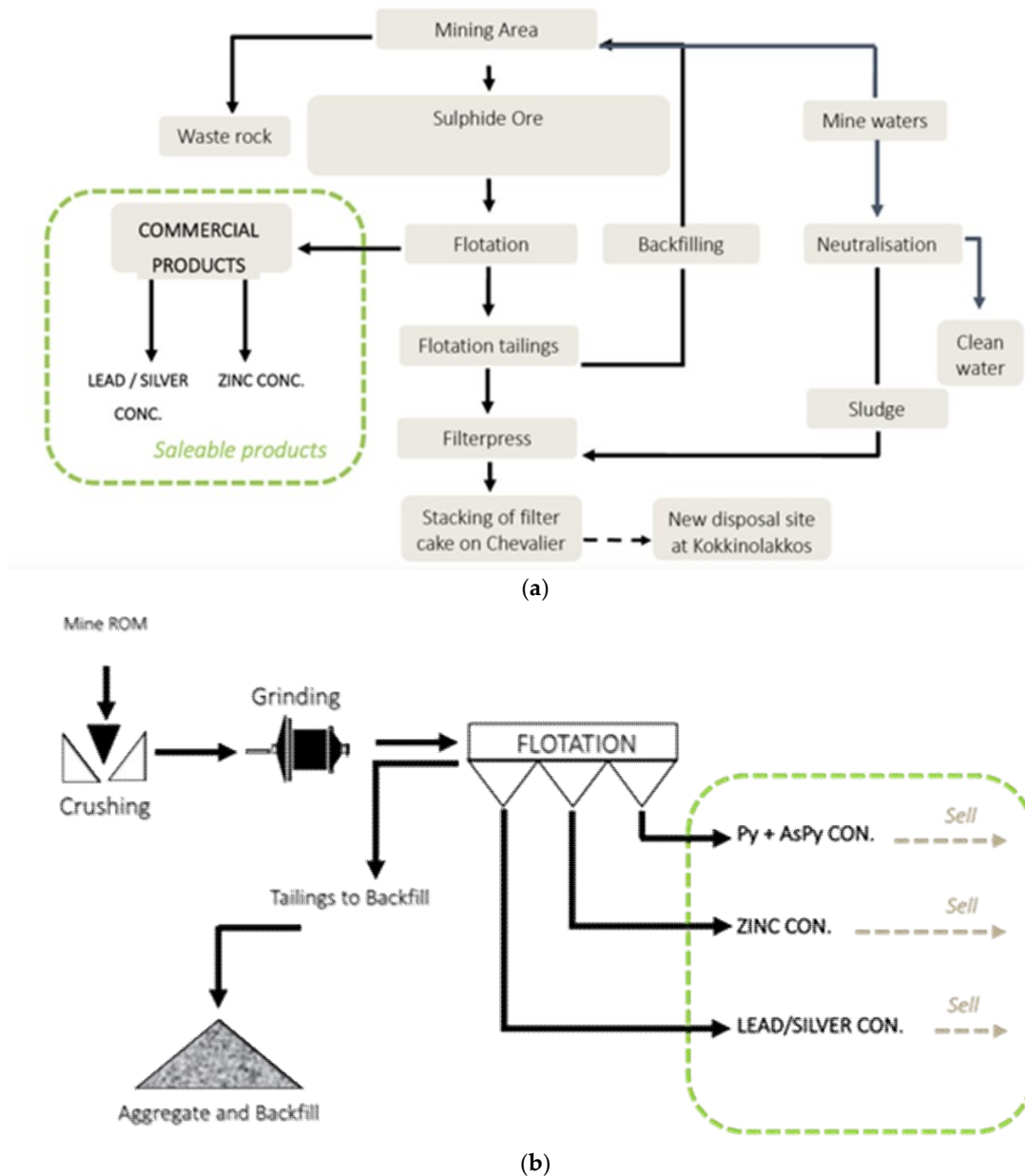
---

37 **1. Introduction**

38 *1.1 Kassandra mines flotation concentrates*

39 The Kassandra mines are located in the Chalkidiki peninsula, Northern Greece. Presently  
40 production is being held in Olympiada mine and Stratoni mines comprising of two deposits;  
41 MademLakkos and MavresPetres. There is a long history of mining in the Kassandra area. It has  
42 been estimated, from the volume of ancient slags, that about 1 million tons of ore were extracted  
43 during the classical Greek period and that the Stratoni mine continued in production through the

44 Roman, Byzantine and Turkish periods. Currently, the Kassandra mines are operated by Hellenic  
 45 Gold S.A. [ 1] and produce Pb (galena), ZnS (sphalerite) and Fe-As-S (pyrite/As-pyrite/arsenopyrite)  
 46 concentrates in two flotation plants, constructed during 70s, at Stratoni and Olympiada areas (Figure  
 47 1). Recently (2018), Olympiada mine has started again the production of concentrates containing Pb,  
 48 Zn, Ag and Au.



49 **Figure 1.** The current flotation plant scheme in Stratoni(a) and Olympiada (b).

50 *1.2 Kassandra deposits and previous work on mineralogy and geochemistry of the concentrates*

51 The Kassandra mining district (Figure 2) contains porphyry Au-Cu and Au-Ag-Pb-Zn-Cu  
 52 carbonate replacement deposits that are associated with Oligocene-Miocene intrusions emplaced  
 53 into poly-deformed metamorphic basement rocks belonging to the Permo-Carboniferous to Late  
 54 Jurassic Kerdilion unit and the Ordovician-Silurian Vertiskos unit. Regional extensional tectonics  
 55 active since the middle Eocene resulted in the development of widespread normal and

56 transtensional faults, including the Stratoni fault zone that hosts carbonate replacement sulfide ore  
57 bodies [ 2] . More particularly, Stratoni (MademLakkos, MavresPetres) and Olympiada are the two  
58 main carbonate-replacement massive sulphidePb-Zn (Ag-Au) deposits of the district; they are  
59 located on the footwall of the Tertiary Stratoni-Varvara fault. Both deposits are interpreted to form  
60 the proximal and distal part of a fault-controlled exoskarn-type ore system triggered by nearby  
61 small-scale intrusions close to the fault system [ 3] Sulphide mineralization occurs within  
62 amphibolite grade metamorphic rocks of the Kerdylia assemblage. The assemblage represents  
63 ametamorphosed marine sedimentary-volcanic sequence of probable Mesozoic or older age. Eocene  
64 and Oligocene age granitic intrusions occur throughout the Kerdylia sequence, mainly as pegmatite  
65 and granite dykes of several generations that range from syn- to post-metamorphic in age. The  
66 sequence is affected by syn-peak metamorphic penetrative deformation that is manifested by  
67 adominant, shallow dipping layer-parallel foliation. At least two other foliation-forming events  
68 affect the sequence with progressively less strain, as well as significant late extensional faulting.

69 Previous workers [ 4] have interpreted the area to lie at the southwestern margin of the  
70 Rhodope complex, and that the shallow dipping foliations which are present formed in response to  
71 Tertiary unroofing of the Rhodope Complex as a metamorphic core complex. In such an  
72 interpretation, the Stratoni Fault has been interpreted as the principal detachment fault forming the  
73 southern major bounding structure between the Rhodope complex, represented locally by the  
74 Kerdylia sequence, and the Vertiskos Formation to the south.

75 Other interpretations suggest that the fabrics are contractional and that the fault may  
76 remobilize a major reverse structure that superimposed the Vertiskos sequence against the Kerdylia.  
77 Geological relationships suggest that the metamorphic fabrics represent contractional rather than  
78 extensional fabrics, and the Stratoni Fault as is currently manifested is dominantly a later, lower  
79 greenschist grade extensional structure that is superimposed onto the amphibolite grade fabrics.

80 Mineralization at Olympiada and Stratoni (M. Lakkos-MavresPetres) is of carbonate  
81 replacement. It occurs in association with a marble horizon. Mineralization is structurally late in  
82 timing and is superimposed on the metamorphic fabrics in the area and in association with an  
83 extensional, brittle to semi-brittle fault network that was likely active coevally with the ore-hosting  
84 Stratoni Fault to the south.

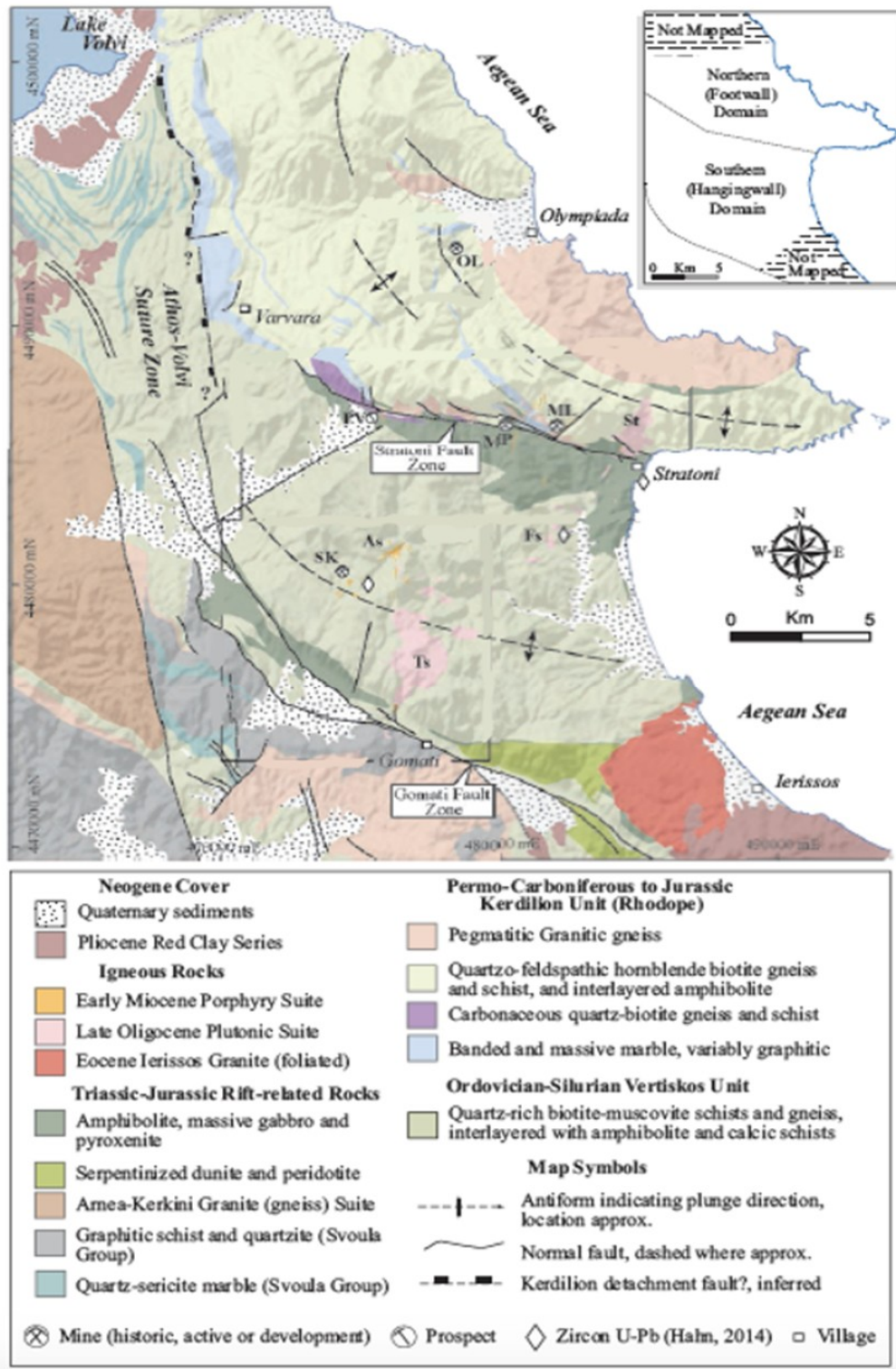


Figure 2. Geological map of the area of NE Calkidiki [ 2 and references therein] .

85

86

87

88

89

90

91

Previous works on mineralogy and geochemistry of ores, derived from both Stratioti (MademLakkos-Mavres Peters) and Olympias mines, have been presented in the literature (e.g [ 2, 3, 9-15] ). However, there is very limited literature about the flotation concentrates (e.g. [ -26] ) and particularly with respect to their mineral chemistry issues and moreover trace and critical element content.

### 92 1.3 Scope of the present study

93 As mentioned above, there are few published works about the concentrates, produced by  
94 Kassandra mines since 70s. Additionally, on the best of our knowledge, there are no published data  
95 about trace and critical elements in these hydrometallurgy (flotation) products. Thus, the scope of  
96 the present study, was to demonstrate new results concerning: i) the mineral chemistry and the  
97 formulae of the sulfide minerals into the concentrates, ii) the trace and critical element content,  
98 specifically REE, Sb, Bi, Ge, V, Ga, Co (e.g. BGS), iii) the actinide element content (U, Th) as well as  
99 their natural radioactivity. Radioisotopes present in the environment can be classified as naturally  
100 occurring and are components of the earth's crust since its formation (e.g.  $^{238}\text{U}$ ,  $^{235}\text{U}$ ,  $^{232}\text{Th}$  and their  
101 decay products as well as  $^{40}\text{K}$ ), cosmogenic radioisotopes (radioisotopes that are produced by the  
102 interaction between cosmic radiation and the atmosphere (e.g.  $^{14}\text{C}$ ,  $^{10}\text{Be}$ ,  $^{44}\text{Ti}$  and  $^{22}\text{Na}$ ) and finally  
103 artificially produced radionuclides that are produced in nuclear reactors (e.g.  $^{90}\text{Sr}$  and  $^{137}\text{Cs}$ ). Natural  
104 radionuclides can be found in soil, rocks, water, air, food, building materials, etc. The study of  
105 natural radioactivity present in geological materials and ores is an important subject in  
106 environmental radiological protection as it provides the possibility to assess any associated health  
107 hazard. In this paper, the products of the Kassandra mines are studied for their natural radioactivity.  
108 This involves not only the products themselves, but the associated risk from mine tailings (surface  
109 water) and dissolution from underground water. Moreover, the results are explained by bulk  
110 geochemistry of the samples.

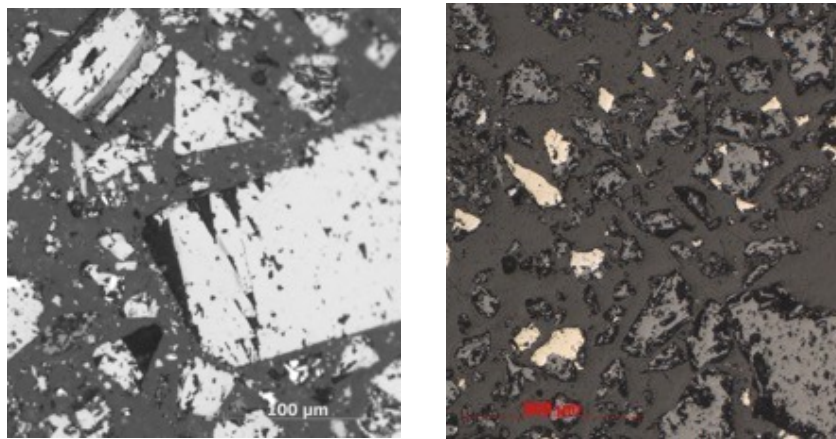
## 111 2. Materials and Methods

### 112 2.1 Samples

113 Representative composite pyrite/As-pyrite/arsenopyrite (Py-(As)Py-AsPy), galena (PbS) and  
114 sphalerite (ZnS) concentrates -in powdered form-, from the flotation plants of Olympiada and  
115 Stratoni (Kassandra mines, Chalkidiki, N. Greece), were supplied by Hellas Gold S.A.

### 116 2.2 Point analyses

117 Scanning electron microscopy (SEM) images of free mineral grains and microprobe analyses  
118 (EPMA) on polished mineral grains (after examination in optical microscope -see Figure 3-) were  
119 obtained using a J EOL 8200 electron probe micro-analyzer equipped with a wavelength dispersive  
120 spectrometer (WDS). Analytical conditions were: 15kV accelerating voltage, 15 nA beam current, 2  
121  $\mu\text{m}$  beam diameter with a counting time of 20 s on the peaks and 10 s on the background.



122 **Figure 3.** Optical images (reflected light) of polished minerals grains in Stratoni PbS and ZnS  
123 concentrates.

124

### 125 2.3 Bulk analyses

126 Major and trace elements, in the powdered concentrates, were analyzed using a Perkin Elmer  
127 ICP-OES and a Perkin Elmer Sciex Elan 9000 ICP-MS following a  $\text{LiBO}_2/\text{LiB}_4\text{O}_7$  fusion and  $\text{HNO}_3$   
128 digestion of the fused solid sample.

### 129 2.4 Gamma-ray spectroscopy

130 The samples after oven-dried at  $60^\circ\text{C}$  to constant weight, were measured using two  
131 high-resolution gamma ray spectrometry systems. The first one consisted of an HPGe coaxial  
132 detector with 42% efficiency and 2.0 keV resolution at 1.33 MeV photons, shielded by 4" Pb, 1mm Cd  
133 and 1mm Cu and the second one consisted of a LEGe planar detector with 0.7 keV resolution at 122  
134 keV photons, shielded by 3.3" Fe-Pb, 1mm Cd and 1mm Cu. The first spectrometry system with the  
135 High Purity Ge detector was used to measure the majority of the natural radionuclides examined in  
136 this study, except  $^{238}\text{U}$ . The second one with the Low Energy planar Ge detector was used so as to  
137 determine only the concentration of  $^{238}\text{U}$ , considering the low energy  $\gamma$ -ray of 63 keV emitted by its  
138 daughter  $^{234}\text{Th}$ .

139 The  $^{40}\text{K}$  content was obtained using its 1461 keV  $\gamma$ -ray. The  $^{232}\text{Th}$  content was calculated as the  
140 weighted mean value of  $^{228}\text{Ra}$  concentration (measured as  $^{228}\text{Ac}$ , using 911, 968 and 338 keV  $\gamma$ -rays)  
141 and  $^{228}\text{Th}$  concentration (measured as decay products in equilibrium, i.e.  $^{212}\text{Pb}$ , using 238 and 300 keV  
142  $\gamma$ -rays,  $^{212}\text{Bi}$ , using 727 keV  $\gamma$ -ray and  $^{208}\text{Tl}$ , using 2614, 583 and 860 keV  $\gamma$ -rays). The determination of  
143  $^{226}\text{Ra}$  content was based on measurement of  $^{222}\text{Rn}$  decay products being in equilibrium. The  
144 measurement of  $^{226}\text{Ra}$  from its own  $\gamma$ -ray at 186.25 keV introduces some problems because of the  
145 adjacent photo peak of  $^{235}\text{U}$  at 185.75 keV, so that the isotopic ratio between  $^{235}\text{U}$  and  $^{238}\text{U}$  was  
146 considered being the natural one, i.e. 0.0072 and secular equilibrium between  $^{238}\text{U}$  and  $^{226}\text{Ra}$  had to be  
147 assumed. Accuracy in the measurements of  $^{226}\text{Ra}$  concentrations by  $^{222}\text{Rn}$  decay products depended  
148 on the integral trapping of radon gas in the sample volume, so a small addition (~2%) of charcoal in  
149 powder form (less than 400  $\mu\text{m}$  in size) was mixed with the sample before sealing it hermetically and  
150 storing it in a freezer during  $^{222}\text{Rn}$  in-growth period [ 21] . The efficiency calibration of the gamma  
151 spectrometry systems was performed with the radionuclide specific efficiency method in order to  
152 avoid any uncertainty in gamma ray intensities as well as the influence of coincidence summation  
153 and self-absorption effects of the emitting gamma photons. A set of high quality certified reference  
154 materials (RGU-1, RGTh-1, RGK-1) [ 22] was used, with densities similar to the average beach sands  
155 measured after pulverization. Cylindrical geometry was used assuming that the radioactivity is  
156 homogenously distributed in the measuring samples. The samples were measured up to 200.000 s in  
157 order to achieve a Minimum Detectable Activity of 12 Bq  $\text{kg}^{-1}$  for  $^{40}\text{K}$ , 4 Bq  $\text{kg}^{-1}$  for  $^{232}\text{Th}$ , 2 Bq  $\text{kg}^{-1}$  for  
158  $^{228}\text{Th}$ , 2 Bq  $\text{kg}^{-1}$  for  $^{226}\text{Ra}$  and 21 Bq  $\text{kg}^{-1}$  for  $^{238}\text{U}$ , with 33% uncertainty. The total uncertainty of the  
159 radioactivity levels was calculated by propagation of the systematic and random errors of  
160 measurements. The systematic errors in the efficiency calibration ranges from 0.3–2% and the  
161 random errors of the radioactivity measurements extend up to 19 %, except in the  $^{238}\text{U}$  measurement,  
162 where the error extends up to 50% for activities measured lower 10 Bq  $\text{kg}^{-1}$ .

## 163 3. Results and Discussion

### 164 3.1 Mineral chemistry

165 The SEM and EPMA data, concerning the mineral chemistry of the sulfide minerals (major  
166 phases) into the concentrates from the flotation plants of Stratoni and Olympiada mines, are given in  
167 Figures 4-6 and Tables 1-3.

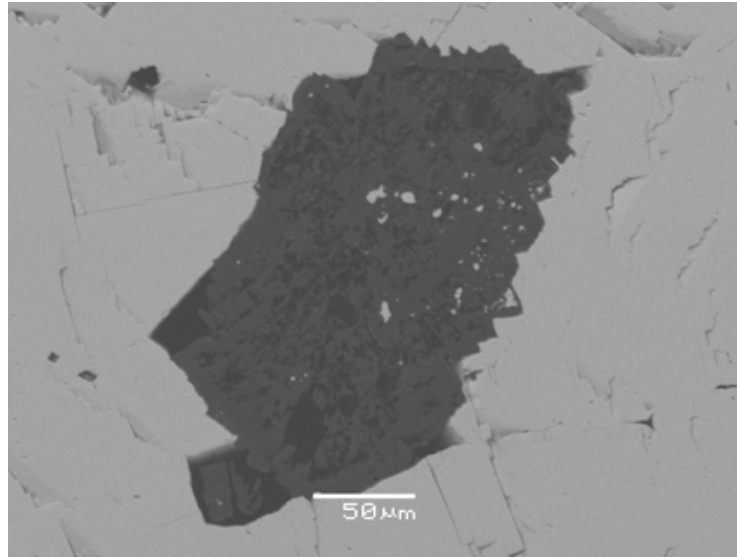
168 The chemical formulae of the major sulfide minerals were calculated as following:

- 169 • Galena (Stratoni):  $\text{Pb}_{0.98-0.99}\text{S}$
- 170 • Sphalerite (Stratoni):  $\text{Zn}_{0.79-0.85}\text{Fe}_{0.12-0.17}\text{Mn}_{0.00-0.01}\text{S}$
- 171 • Pyrite (Olympiada):  $\text{Fe}_{1.02-1.05}\text{As}_{0.00-0.03}\text{S}_2$
- 172 • Arsenopyrite (Olympiada):  $\text{FeAs}_{0.85-0.88}\text{S}_{1.07-1.13}$

173 In addition, the frequent presence of boulangerite was confirmed in the Olympiada concentrate.  
174 The EPMA revealed the following chemical formula:

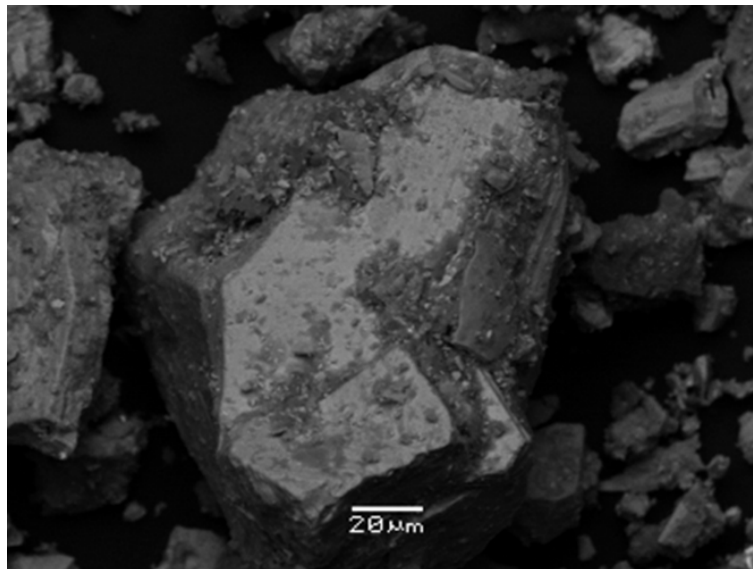
175 • Boulangerite (Olympiada):  $\text{Pb}_{5.18-5.25}\text{Sb}_{4.21-4.45}\text{As}_{0.06-0.15}\text{Fe}_{0.04-0.15}\text{Zn}_{0.00-0.06}\text{Mn}_{0.01-0.02}\text{S}_{11}$

176 All sulfide minerals studied were found to exhibit typical/expected chemical compositions in  
177 major elements. Ongoing research on these samples is also targeting the characterization of noble  
178 metals [ 19, 23] .



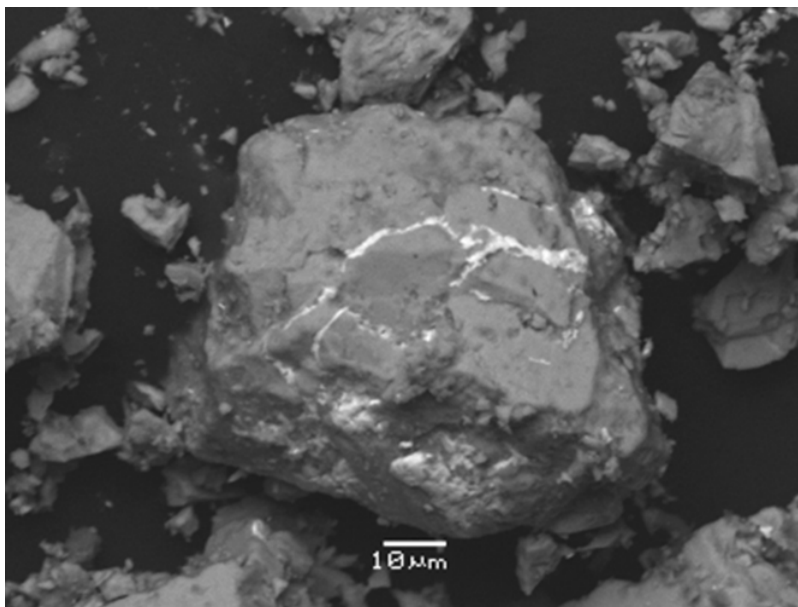
179

180 **Figure 4.** BSE image of polished galena, with carbonate mineral inclusions, in Stratoni PbS  
181 concentrate.



182

183 **Figure 5.** BSE image of free pyrite grain (darker), including arsenopyrite (brighter), in Olympiada  
184 Py-(As)Py-AsPy concentrate.



185

186

**Figure 6.** BSE image of free sphalerite grain, with galena veins, in Stratoni ZnS concentrate.



**Table 1.** EPMA analyses of mineral phases present in Stratoni ZnS concentrate.

Phase Endmember AnalysisNo.	Sphalerite (Zn,Fe)S						Galena PbS		Arsenopyrite FeAsS	Pyrite FeS <sub>2</sub>		
	2	3	4	15	16	17	10	11	1	5	6	7
<b>As</b>	0.03	0.00	0.00	0.00	0.01	0.02	0.00	0.01	42.08	1.08	1.40	1.24
<b>Fe</b>	8.35	7.05	10.07	8.37	8.22	7.48	0.46	0.08	36.07	47.54	47.56	47.12
<b>Mn</b>	0.58	0.61	0.38	0.43	0.57	0.49	0.00	0.00	0.00	0.06	0.00	0.02
<b>Pb</b>	0.00	0.06	0.14	0.05	0.08	0.02	85.91	84.86	0.08	0.12	0.02	0.16
<b>S</b>	34.37	34.33	34.59	34.52	34.42	34.53	13.33	13.38	22.37	52.76	52.58	53.12
<b>Zn</b>	56.84	59.13	55.58	57.04	57.71	58.24	0.79	0.28	1.33	0.07	0.53	0.28
<b>Total</b>	100.18	101.18	100.75	100.41	101.01	100.79	100.48	98.61	101.94	101.63	102.09	101.95
<b>Ionsbasedon:</b>	1 (S)						1 (S)		1 (Fe)	2 (S)		
<b>As</b>	---	---	---	---	---	---	---	---	0.87	0.02	0.02	0.02
<b>Fe</b>	0.14	0.12	0.17	0.14	0.14	0.12	0.02	---	1.00	1.03	1.04	1.02
<b>Mn</b>	0.01	0.01	0.01	0.01	0.01	0.01	---	---	---	---	---	---
<b>Pb</b>	---	---	---	---	---	---	1.00	0.98	---	---	---	---
<b>S</b>	1.00	1.00	1.00	1.00	1.00	1.00	1.00	1.00	1.08	2.00	2.00	2.00
<b>Zn</b>	0.81	0.84	0.79	0.81	0.82	0.83	0.03	0.01	0.03	---	0.01	0.01

**Table 2.** EPMA analyses of mineral phases present in Stratoni PbS concentrate

Phase Endmember AnalysisNo.	Galena PbS						Arsenopyrite FeAsS				Pyrite FeS <sub>2</sub>			
	1	4	5	6	13	14	2	7	8	9	3	10	11	12
<b>As</b>	0.04	0.01	0.03	0.03	0.03	0.02	41.53	42.43	41.60	43.41	1.03	0.11	2.03	1.92
<b>Fe</b>	0.00	0.00	0.00	0.00	0.00	0.00	36.52	36.22	36.55	36.04	47.12	47.71	47.19	47.03
<b>Mn</b>	0.02	0.02	0.00	0.04	0.03	0.01	0.01	0.02	0.04	0.00	0.03	0.04	0.00	0.05
<b>Pb</b>	86.33	85.87	85.66	85.76	85.92	86.12	0.17	0.10	0.16	0.00	0.16	0.14	0.15	0.21
<b>S</b>	13.61	13.42	13.56	13.54	13.52	13.67	23.72	22.46	23.02	22.05	53.15	53.69	52.04	52.67
<b>Zn</b>	0.00	0.02	0.12	0.00	0.08	0.00	0.18	0.06	0.08	0.00	0.02	0.08	0.00	0.05
<b>Total</b>	100.01	99.33	99.37	99.37	99.58	99.82	102.13	101.29	101.45	101.50	101.50	101.76	101.41	101.93
<b>Ionsbasedon:</b>	1 (S)						1 (Fe)				2 (S)			
<b>As</b>	---	---	---	---	---	---	0.85	0.87	0.85	0.90	0.02	---	0.03	0.03
<b>Fe</b>	---	---	---	---	---	---	1.00	1.00	1.00	1.00	1.02	1.02	1.04	1.03
<b>Mn</b>	---	---	---	---	---	---	---	---	---	---	---	---	---	---
<b>Pb</b>	0.98	0.99	0.98	0.98	0.98	0.98	---	---	---	---	---	---	---	---
<b>S</b>	1.00	1.00	1.00	1.00	1.00	1.00	1.13	1.08	1.10	1.07	2.00	2.00	2.00	2.00
<b>Zn</b>	---	---	---	---	---	---	---	---	---	---	---	---	---	---

**Table 3.** EPMA analyses of mineral phases present in Olympiada Py-(As)Py-AsPy concentrate

Phase Endmember AnalysisNo.	Sphalerite (Zn,Fe)S	Boulangerite Pb <sub>5</sub> Sb <sub>4</sub> S <sub>11</sub>			Arsenopyrite FeAsS						Pyrite FeS <sub>2</sub>					
	1	13	14	15	2	3	16	17	18	20	5	6	7	19	21	22
<b>As</b>	0.00	0.22	0.58	0.35	41.02	41.35	41.07	41.22	41.43	41.18	2.03	0.02	1.43	0.89	1.68	1.24
<b>Fe</b>	11.28	0.11	0.43	0.15	36.41	36.77	36.52	36.55	36.85	36.57	47.42	47.82	47.25	47.55	47.74	47.33
<b>Mn</b>	0.61	0.03	0.06	0.06	0.03	0.02	0.03	0.03	0.22	0.23	0.00	0.00	0.00	0.00	0.00	0.00
<b>Pb</b>	0.10	54.76	54.38	56.25	0.04	0.07	0.05	0.06	0.05	0.04	0.17	0.14	0.12	0.15	0.13	0.16
<b>S</b>	34.55	17.99	17.66	18.23	23.47	22.73	22.84	23.15	22.36	22.94	52.03	53.90	52.45	53.11	52.17	52.41
<b>Zn</b>	53.64	0.21	0.05	0.00	0.10	0.16	0.13	0.15	0.17	0.15	0.00	0.04	0.00	0.03	0.00	0.02
<b>Sb</b>	n/a <sup>1</sup>	27.08	27.12	26.51	n/a	n/a	n/a	n/a	n/a	n/a	n/a	n/a	n/a	n/a	n/a	n/a
<b>Total</b>	100.17	100.40	100.27	101.55	101.07	101.10	100.64	101.16	101.08	101.10	101.65	101.92	101.25	101.74	101.72	101.16
<b>Ionsbasedon:</b>	1 (S)	11 (S)			1 (Fe)						2 (S)					
<b>As</b>	---	0.06	0.15	0.09	0.84	0.84	0.84	0.84	0.84	0.84	0.03	---	0.02	0.01	0.03	0.02
<b>Fe</b>	0.19	0.04	0.15	0.05	1.00	1.00	1.00	1.00	1.00	1.00	1.05	1.02	1.03	1.03	1.05	1.04
<b>Mn</b>	0.01	0.01	0.02	0.02	---	---	---	0.00	0.01	0.01	---	---	---	---	---	---
<b>Pb</b>	---	5.18	5.24	5.25	---	---	---	---	---	---	---	---	---	---	---	---
<b>S</b>	1.00	11.00	11.00	11.00	1.12	1.08	1.09	1.10	1.06	1.09	2.00	2.00	2.00	2.00	2.00	2.00
<b>Zn</b>	0.76	0.06	0.01	---	---	---	---	---	---	---	---	---	---	---	---	---
<b>Sb</b>	n/a	4.36	4.45	4.21	n/a	n/a	n/a	n/a	n/a	n/a	n/a	n/a	n/a	n/a	n/a	n/a

<sup>1</sup>n/a=not analyzed.

## 192 3.2 Geochemistry

193 The bulk chemical compositions (ICP-OES & MS) of the studied Kassandra mines concentrates  
 194 are given in Table 4. It is obvious that basic and noble metals (Pb, Zn, Ag, and Au) being exploited by  
 195 Hellas Gold S.A., show high concentrations, as well as Sb and Ga (Sb: >0.2 wt.% in PbS concentrate;  
 196 Ga: 25 ppm in ZnS concentrate). On the other hand, there are no considerable contents of Bi, Co, V,  
 197 and REE. Considering other elements, As is found in elevated concentrations (>1 wt.% in  
 198 Py-(As)Py-AsPyOlympiada concentrate and almost 1 wt.% in StratoniPbS and ZnS concentrates)  
 199 along with Cd (specifically in ZnS concentrate). Moreover, actinides occur in very low  
 200 concentrations (U <2 ppm and Th<0.5 ppm in all concentrates).

201 The enrichment and depletion of the elements studied can be revealed from the normalization  
 202 to the Upper Crust (UCC) (Figure 7), the Primitive Mantle (Figure 8) and the Chondrite (Figure 9).  
 203 REE's and other elements like Cs, Rb, Co, Ni, Ba and V are depleted. As expected, major elements  
 204 like Pb, Zn and Cu are enriched, as well as other trace elements like Mo, As, Sb, Se, Sn, Cd, Hg, Rb  
 205 and U. It should be noted that the enrichment in these trace elements, relative to UCC, Primitive  
 206 Mantle and Chondrite, is strictly geochemical and it is not associated to practical mining and  
 207 metallurgical issues. For instance, if we consider U, the bulk natural radioactivity of the samples is  
 208 negligible, as discussed below.

 209 **Table 4.** Trace and critical elements concentration of the studied Kassandra mines concentrates.

Element	MDL (ppm)	Py-(As)Py-AsPy Conc.	PbS Conc.	ZnS Conc.
		OLYMPIADA	STRATONI	STRATONI
Pb	0.1	5235.9	>10000.0	>10000.0
Zn	1	>10000	>10000	>10000
Ag	0.1	22.5	>100.0	>100.0
Au	0.0005	16.9	1.1	1.0
Cu	0.1	710.8	1035.9	2191.1
As	0.5	>10000.0	>10000.0	9476.9
Sb	0.1	712.9	>2000.0	748.2
Bi	0.1	0.1	2.0	0.2
Cd	0.1	54.5	77.7	>2000.0
Ni	0.1	9.3	6.6	3.1
Co	0.2	1.7	0.5	0.2
Hg	0.01	0.15	0.49	10.98
Tl	0.1	1.2	37.2	3.4
Se	0.5	2.7	8.3	<0.5
Be	1	<1	<1	<1
Th	0.2	0.5	<0.2	<0.2
U	0.1	1.4	2.0	1.1
Sn	1	43	131	218
Mo	0.1	2.6	29.9	5.7
Ga	0.5	4.5	1.5	25.4
V	8	12	9	<8
Nb	0.1	1.0	<0.1	<0.1
Ta	0.1	<0.1	<0.1	<0.1

---

W	0.5	1.8	1.0	0.7
Ba	1	15	8	2
Cs	0.1	0.4	0.2	0.3
Hf	0.1	0.2	<0.1	<0.1
Rb	0.1	6.9	2.1	3.1
Sr	0.5	7.1	1.5	1.9
Zr	0.1	3.9	2.0	1.9
Y	0.1	0.5	0.2	0.1
La	0.1	1.2	<0.1	0.4
Ce	0.1	2.0	0.8	1.1
Pr	0.02	0.20	0.09	0.10
Nd	0.3	0.8	<0.3	<0.3
Sm	0.05	0.12	<0.05	<0.05
Eu	0.02	0.03	<0.02	<0.02
Gd	0.05	0.16	<0.05	0.08
Tb	0.01	0.02	<0.01	<0.01
Dy	0.05	0.10	<0.05	<0.05
Ho	0.02	<0.02	<0.02	<0.02
Er	0.03	0.04	<0.03	<0.03
Tm	0.01	0.01	<0.01	<0.01
Yb	0.05	<0.05	<0.05	<0.05
Lu	0.01	0.01	<0.01	<0.01

---

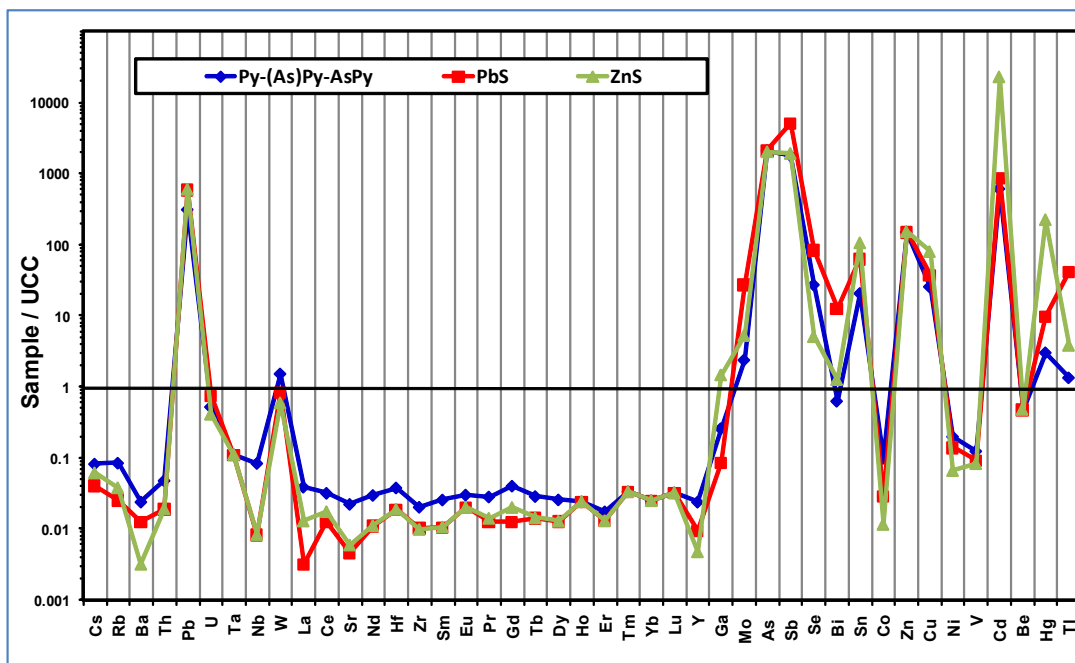


Figure 7. Spider diagram of Sample/Upper Continental Crust (UCC).

210

211

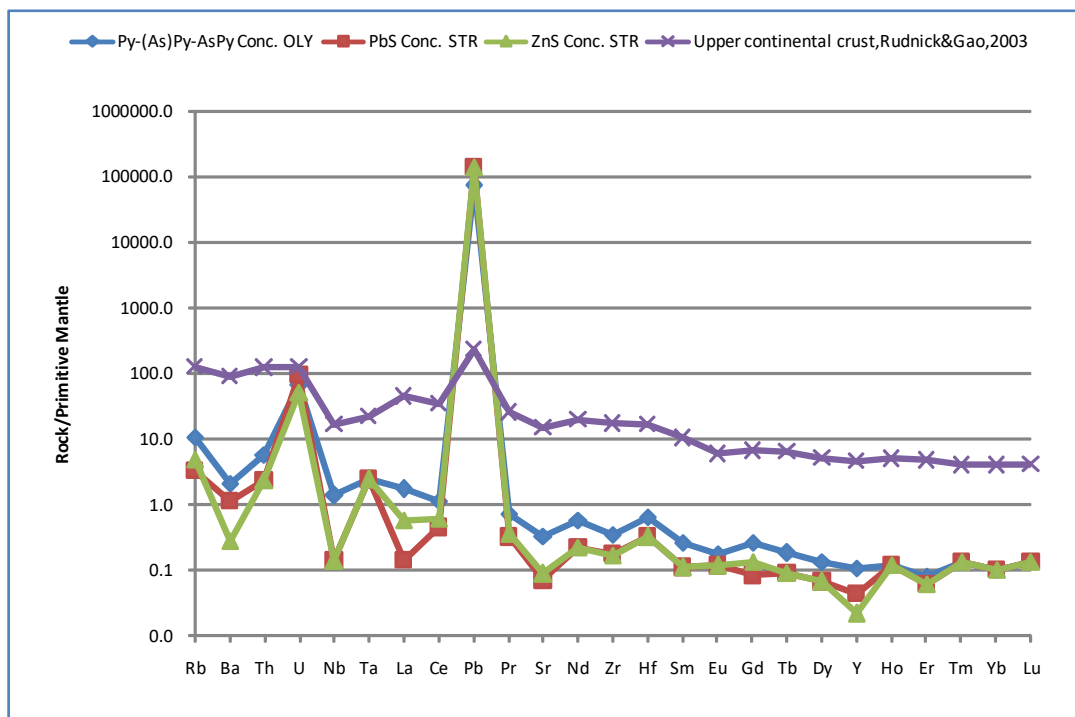


Figure 8. Spider diagram of Sample/Primitive Mantle.

212  
213

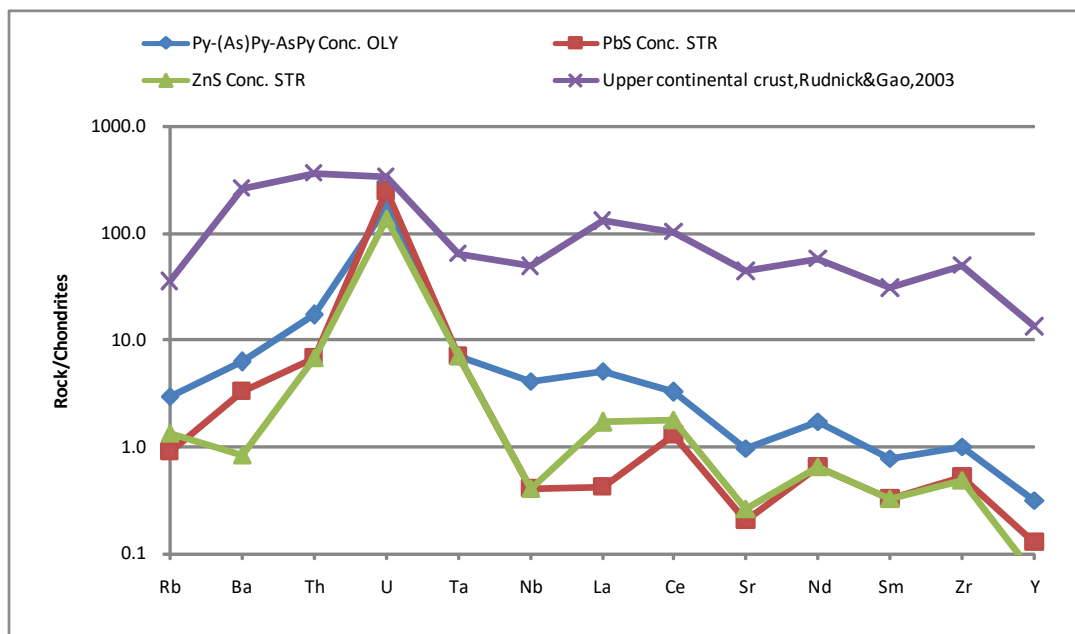


Figure 9. Spider diagram of Sample/Chondrite.

214  
215



### 216 3.3 Actinide elements and natural radioactivity

217 The concentrations of the natural radionuclides, detected by gamma-ray spectroscopy, are  
218 given in Table 5.

219 **Table 5.** Activity concentrations of  $^{238}\text{U}$ ,  $^{226}\text{Ra}$ ,  $^{232}\text{Th}$ ,  $^{228}\text{Th}$  and  $^{40}\text{K}$  ( $\text{Bq.kg}^{-1}$ ), along with the respective  
220 standard errors ( $\pm\sigma$ ).

Sample	$^{238}\text{U}$ -series				$^{232}\text{Th}$ -series				$^{40}\text{K}$		$^{226}\text{Ra}$	$^{232}\text{Th}$
	$^{238}\text{U}$		$^{226}\text{Ra}$		$^{232}\text{Th}$		$^{228}\text{Th}$		$^{40}\text{K}$		$^{226}\text{Ra}$	$^{232}\text{Th}$
	$\text{Bq.kg}^{-1}$	$\pm\sigma$	$\text{Bq.kg}^{-1}$	$\pm\sigma$	$\text{Bq.kg}^{-1}$	$\pm\sigma$	$\text{Bq.kg}^{-1}$	$\pm\sigma$	$\text{Bq.kg}^{-1}$	$\pm\sigma$	ppm	ppm
OLY-C-(FeAsS)	B.D.L.	-	24.8	0.3	4.1	0.7	3.3	0.2	51.5	2.9	2.0	1.0
STR-(PbS)	B.D.L.	-	22.0	0.3	1.0	0.5	B.D.L.	-	10.8	2.1	1.8	0.2
STR-(ZnS)	B.D.L.	-	19.1	0.4	1.3	0.8	B.D.L.	-	18.2	2.8	1.5	0.3

221 The concentrations of the radionuclides of  $^{238}\text{U}$ ,  $^{232}\text{Th}$ -series and  $^{40}\text{K}$  are small and close to the  
222 detection limit of gamma-ray spectroscopy. These small concentrations are mainly due to the small  
223 ability of the chemical components of the sulphides to be substituted by the measured radionuclides.  
224 Moreover, low concentrations of these radionuclides have been detected in the Stratoni granitic  
225 bodies [ 24] . Similar conclusions on the content of sulphides have been previously reported by [ 25,  
226 26] . However, the previous researchers mention that high U concentrations may be present in the  
227 late accessory mineral phases deposited in microfissures.

228 These values are by far lower than a typical granitic rock used as building material [ 26] .  
229 Therefore, the radioactive dose to humans from these materials is insignificant.

## 230 4. Conclusions

231 The results of the present study can be summarized as follows:

- 232 • Except basic (Pb, Zn, and potentially Cu) and noble (Ag, Au) elements in Kassandra mines  
233 concentrates, being exploited and commercialized by Hellas Gold S.A., it can be argued that  
234 there are also significant concentrations of Sb and Ga (Sb: >0.2 wt.% in PbS concentrate; Ga: 25  
235 ppm in ZnS concentrate), but no substantial contents of Bi, Co, V, and REE.
- 236 • Concerning other elements, of course it well-known that As occurs in rather high concentrations  
237 (>1 wt.% in Py-(As)Py-AsPy Olympias concentrate and almost 1 wt.% in Stratoni PbS and ZnS  
238 concentrates), as well as Cd (specifically in ZnS concentrate).
- 239 • There are negligible concentrations of actinides ( $\text{U} < 2$  ppm and  $\text{Th} < 0.5$  ppm in all concentrates),  
240 minimizing the possibility of increased natural radioactivity. The concentrations of natural  
241 radionuclides are by far lower than a typical granitic rock used as building material  
242 (Papadopoulos et al. 2013). Therefore, the radioactive dose to humans from these materials is  
243 insignificant.

244 **Author Contributions:** E. Tzamos, in collaboration with A. Papadopoulos and S. Stoulos, participated in data  
245 acquisition and wrote the original draft paper; G. Grieco and M. Bussolesi contributed to data acquisition and  
246 validated the paper; E. Daftsis and E. Vagli reviewed and edited the original draft paper; D. Dimitriadis with A.  
247 Godelitsas administrated & supervised the entire paper.

248 **Funding:** This research received no external funding

249 **Acknowledgments:** This research is implemented through IKY scholarships programme and co-financed by  
250 the European Union (European Social Fund - ESF) and Greek national funds through the action  
251 entitled "Reinforcement of Postdoctoral Researchers", in the framework of the Operational  
252 Programme "Human Resources Development Program, Education and Lifelong Learning" of the National  
253 Strategic Reference Framework (NSRF) 2014 – 2020.

254 **Conflicts of Interest:** The authors declare no conflict of interest.

255 **References**

- 256 1. Available online at: <https://www.hellas-gold.com/>
- 257 2. Siron, C.; Rhys, D.; Thompson, J.; Baker, T.; Veligrakis, T.; Camacho, A.; Dalampiras, L. Structural
- 258 Controls on Porphyry Au-Cu and Au-Rich Polymetallic Carbonate-Hosted Replacement Deposits of
- 259 the Kassandra Mining District, Northern Greece. *Economic Geology*, 2018, 113 (2), 309-345.
- 260 3. Hahn, A.; Naden, J.; Treloar, P.J.; Kiliass, S.P.; Rankin, A.H.; Forward, P. A new timeframe for the
- 261 mineralization in the Kassandra mine district, N. Greece: Deposit formation during metamorphic core
- 262 complex exhumation. 2012, *European Mineralogical Conference*, v. 1, 1EMC2012-742.
- 263 4. Kocke, I. F.; Mollat, H.; Walther, H.W. *Geologie des Serbo-Mazedonischen Massivs und seines*
- 264 *mesozoischen Rahmens (Nordgriechenland)*, 1971, *Geol. J. b.*, 89 (1), 529-551.
- 265 5. Himmerkus, F.; Reischmann T.; Kostopoulos D. Serbo-Macedonian revisited: A Silurian basement
- 266 terrane from northern Gondwana in the Internal Hellenides, Greece, 2009a, *Tectonophysics*, 473(1-2),
- 267 20-35
- 268 6. Himmerkus, F.; Reischmann T.; Kostopoulos D. Triassic rift-related meta-granites in the Internal
- 269 Hellenides, Greece, 2009b, *Geol. Mag.*, 146(2), 252-265,
- 270 7. Himmerkus, F.; Zachariadis, P.; Reischmann T.; Kostopoulos, D. The basement of the Mount Athos
- 271 peninsula, northern Greece: Insights from geochemistry and zircon ages, 2012, *Int. J. Earth Sci.*
- 272 (*GeolRundsch*), 101(6), 1467-1485
- 273 8. Brun, J. P.; Sokoutis D. Kinematics of the Southern Rhodope Core Complex (North Greece), 2007, *Int. J.*
- 274 *Earth Sci. (GeolRundsch)*, 96(6)
- 275 9. Sagui, C.L. The ancient mining works of Cassandra, Greece, 1928, *Econ. Geol.* 23, 671-680.
- 276 10. Nicolaou, M.M. L'intrusion granitique dans la region de Stratoni-Olympiadeetsa relation avec la
- 277 metallogenese, 1960, *Annales Geol. des Pays Helleniques*, v. 11, p. 214-265.
- 278 11. Nicolaou, M.M. The mineralogy and micrography of the sulfide ores of Kassandra mines, Greece,
- 279 1964, *Annales Geol. des Pays Helleniques*, v. 16, p. 111-139.
- 280 12. Nicolaou, M.M. Recent research on the composition of the Kassandra Mines Mines orebodies, 1969,
- 281 *Prakt. Academ. Athens*, v. 44, p. 82-93 (in Greek with English summary).
- 282 13. Kalogeropoulos, S.I. Composition of arsenopyrite from the Olympias Pb-Zn massive sulfide deposit,
- 283 Chalkidiki Peninsula, N. Greece, 1984, *Neues Jahrb. Mineral. Monatsh.*, 29600.
- 284 14. Hahn, A. Nature, timing and geodynamic context of polymetallic mineralisation in the Kassandra
- 285 mining district, North Greece, 2014, Unpublished Ph.D. thesis, London, Kingston University, 351 p.
- 286 15. Siron, C.R.; Thompson, J.F.H.; Baker, T.; Friedman, R.; Tsitsanis, P.; Russell, S.; Randall, S.;
- 287 Mortensen, J. Magmatic and metallogenic framework of Au-Cu porphyry and polymetallic
- 288 carbonate-hosted replacement deposits of the Kassandra Mining District, Northern Greece, 2016,
- 289 *Society of Economic Geologists Special Publication 19*, p. 29-55.
- 290 16. [16] Kontopoulos, A.; Stefanakis, M.; Demitriadis. Extraction of gold and silver from ore factory
- 291 arseniferous-pyrite concentrate slabs, 1986, *Soc. Mining Engineers-Metall. Soc. Am. Inst. Mining*
- 292 *Metall. Petroleum Engineers Annual Mtg.*, 115th, New Orleans, Abstracts with Program, p. 59.
- 293 17. Adam, K.N.; Kontopoulos, A.E.; Stefanakis, M.I. Applications of process mineralogy on the treatment
- 294 of Olympias pyrite concentrate slabs, 1989, *Am. Inst. Mining Metall. Petroleum Engineers Mtg.*, 118th,
- 295 Las Vegas, Abstracts with Program, p.140.
- 296 18. Adam, K.; Prevosteau, J.M.; Kontopoulos, A.E.; Stefanakis, M.I.; Martin, E. Applications of process
- 297 mineralogy on the treatment of the Olympias pyrite concentrate slabs, 1990, *Am. Inst. Mining Metall.*
- 298 *Petroleum Engineers Mtg.*, 119th, Salt Lake City, Abstracts with Program, p. 100.
- 299 19. Godelitsas, A.; Tzamos, E.; Filippidis, A.; Sokaras, D.; Weng, T.C.; Grieco, G.; Papadopoulos, A.;
- 300 Stoulos, S.; Gamaletsos, P.; Mertzimekis, T.J.; Daftsis, E.; Dimitriadis, D. New insights into the mineral
- 301 chemistry of Au-bearing pyrite/As-pyrite/arsenopyrite concentrate from Olympias deposit,
- 302 Kassandra mines (Chalkidiki, Greece), 2015, *Goldschmidt Conference*, Prague, Czech Republic,
- 303 16-21/09/2015, Abstracts, 1062.
- 304 20. Tzamos, E.; Grieco, G.; Bussolesi, M.; Papadopoulos, A.; Stoulos, S.; Daftsis, E.; Dimitriadis, D.;
- 305 Gamaletsos, P.; Godelitsas, A.; Filippidis, A. Mineral chemistry of sulphide minerals in concentrates
- 306 of the Kassandra mines (Chalkidiki, Greece), 2018, *XXI International Congress of the CBGA*, Salzburg,
- 307 Austria, September 10-13, Abstracts

- 308 21. Manolopoulou, M.; Stoulos, S.; Mironaki, D.; Papastefanou, C. A new technique for accurate  
309 measurements of Ra-226 with  $\gamma$ -spectroscopy in voluminous samples, 2002, Nucl. Inst. Methods, A,  
310 508, 362-366.
- 311 22. I.A.E.A. Preparation of Gamma-ray Spectroscopy Reference Materials RGU-1, RGTh-1 and RGK-1,  
312 1987, Report-IAEA/RL/148, Vienna.
- 313 23. Kasama, T.; Gamaletsos, P.; Escrig, S.; Wenzell, B.; Jensen, L.; Meibom, A.; Sokaras, D.; Weng, T.C.;  
314 Dimitridis, D.; Godelitsas, A. Nanoscale observations of 'invisible gold' from the Olympias mine,  
315 Greece, 2018, 33rd Nordic Geological Winter Meeting, Lyngby, Denmark, 10-12/01/2018, Abstracts,  
316 133-134.
- 317 24. Papadopoulou, A.; Christofides, G.; Koroneos, A.; Papadopoulou, L.; Papastefanou, C.; Stoulos, S.  
318 Natural radioactivity and radiation index of the major granitic plutons in Greece, 2013, J. Environ.  
319 Radioactiv., 124, 227-238.
- 320 25. Swart, P.K.; Moore F. The concentration of uranium in ore minerals from St. Michael's Mount and  
321 Cligga Head, 1980, Cornwall. Proc. Ussher. Soc., 4:432-436.
- 322 26. Swart, P.K.; Moore, F. The occurrence of uranium in association with cassiterite, wolframite and  
323 sulphide mineralization in the southwest England, 1982, Min. Mag., 46:211-215. Author 1, A.; Author 2,  
324 B. Title of the chapter. In *Book Title*, 2nd ed.; Editor 1, A., Editor 2, B., Eds.; Publisher: Publisher  
325 Location, Country, 2007; Volume 3, pp. 154-196.



© 2019 by the authors. Submitted for possible open access publication under the terms and conditions of the Creative Commons Attribution (CC BY) license (<http://creativecommons.org/licenses/by/4.0/>).

326